Article

Conceptual Design and Simulation of a Self-Adjustable Heaving Point Absorber Based Wave Energy Converter

Tunde Aderinto [1] and Hua Li [2,*]

[1] Sustainable Energy Systems Engineering, Texas A&M University-Kingsville, Kingsville, TX 78363, USA; tundeaderintos@yahoo.com

[2] Mechanical and Industrial Engineering Department, Texas A&M University-Kingsville, Kingsville, TX 78363, USA

* Correspondence: hua.li@tamuk.edu

check for updates

Abstract: Different concepts and methods have been proposed and developed by many researchers to harvest ocean wave energy. In this paper, a new self-adjustable wave energy converter concept is presented, which changes its inertia through ballasting and de-ballasting using sea water. The trigger of ballasting and de-ballasting is controlled by the critical wave period. Therefore, the self-adjustable wave energy converter is able to interact at resonance with the ocean waves at two different resonant bandwidths. Ten years real wave data with hourly resolution from a selected location in Gulf of Mexico was used in this paper to decide the critical wave period and other parameters of the wave energy converter. The annual energy performance of the self-adjustable wave energy converter was also estimated and compared with non-adjustable wave energy converter with similar dimensions. Structural analysis including both static and fatigue analysis was performed on the self-adjustable wave energy converter to determine its survivability with the real ocean wave data. The results show that the self-adjustable wave energy converter is able to capture more energy than non-adjustable wave energy converter, and is able to survive during the hash ocean wave conditions.

Keywords: wave energy converters; heaving point absorber; self-adjustable: design and performance; structural assessment

1. Introduction

The oil crisis in 1973 increased the interests of developing alternative and reliable forms of energy which include renewable energy sources such as wind, solar and wave [1,2]. Renewable energy resources become attractive as they are readily available in every geographical location and are sustainable. Hence, governments and private entities poured considerable amounts of resources into the research and development efforts related to renewable energy [3–5]. Another attractiveness of renewable is that their operations result in less production of greenhouse gas and other poisonous gases into the atmosphere which are adverse to the environment and health of the population [6].

While many studies have shown that ocean wave energy is considered as abundant [7], there exist few commercially operated installations worldwide [8,9]. Nowadays, solar energy and wind energy are competing commercially with traditional energy sources [10]. Ocean wave energy on the other hand has seen little success commercially compared to wind and solar [8]. Some promising wave energy converter (WEC) concepts developed by some organizations have seen little success, and quite a few WECs have actually failed due to profitability issues [11,12] and the high levelized cost of energy (LCOE) [13]. Another challenge facing the commercialization of ocean wave energy is that WECs operate in harsh ocean environments where the ocean wave forces become very crucial to the

survivability of the WECs during extreme weather conditions such as hurricanes [14]. In addition, the highly corrosive nature of the ocean is another big challenge. Although the structural design of WECs can benefit from the current offshore energy industry which includes offshore wind and oil industries [8,15], all these challenges will potentially reduce the stability and operability of WECs.

Among all the WEC concepts, one promising WEC system is the heaving point absorber system, where the oscillatory motion of a heaving buoy through its interaction with the ocean wave drives a power take-off (PTO) mechanism to convert mechanical energy into electrical energy. For an oscillating heaving wave energy system, its motion can be described by the Equation (1) below.

$$(m + A)x(\ddot{t}) = f_d(t) - bx(\dot{t}) - \rho g S x(t) + f_{PTO}(t) + f_a(t) \tag{1}$$

Since the system is linear and the input (incident wave) is represented by a harmonic function of time, the body displacement and the forces upon the body are also harmonic functions of time. The forces and motion may be written as

$$(t) = Xe^{i\omega t}; \; f_d(t) = F_d e^{i\omega t}; \; f_{PTO}(t) = F_{PTO}e^{i\omega t}; \; \rho g S x(t) = F_s e^{i\omega t} \; ; \; b(t) = Be^{i\omega t}$$

where, m = mass; A = added mass; x is displacement; B = radiation damping coefficient; ρ = density; g = acceleration due to gravity; S = cross-sectional area of the body on the free surface plane; f_{PTO} = force due to power take-off; f_d is the excitation force that is zero in calm water; f_a is forces which include viscous forces, dissipation losses, mooring forces, etcetera. X is the amplitude for the buoy displacement. F_d, F_{PTO} and F_s are the excitation force, PTO force and hydrostatic force, respectively. The mooring forces in this study were assumed to be negligible and would not significantly affect the WEC behavior [16].

The independent studies by Buder [17] and Mei [18] described the hydrodynamics of floating heaving WEC systems and the theoretical power capture occurring when the floating body was at resonance with the ocean waves. However, while a typical device has a very narrow band of resonance frequency, the ocean waves are polychromatic in nature spreading across different frequency bands. Therefore, the floating heaving WEC device can only reach its optimal power capture in a very narrow band of ocean wave frequencies.

Different methods have been used to optimize the performance of floating heaving WECs. Some tried to make WECs operate optimally outside their intrinsic resonance period while some tried to reduce losses like viscous damping. Geometrical optimization was also investigated in which changes were made to the WECs' shapes and dimensions [19,20]. Another method was the latching control in which the WEC was held in a fixed position during operation when the velocity was zero and released when its velocity was in phase with the excitation force [21]. Similar to latching was the declutching method, which worked through the power take-off mechanism by switching it on and off to match the velocity with the excitation force [22]. In addition, the model predictive control, an advanced control strategy compared to the passive control methods, was also used, which employed complex algorithms and simulations to achieve the optimization of power absorption by the WECs [23]. Some researchers also proposed modifying the inertial behavior of the device so that it could absorb power at both high amplitude and low amplitude wave regimes [24].

Similar to any other energy systems, ocean wave energy systems have three stages: (1) The absorbing stage when energy is absorbed from the primary energy source; (2) the conversion stage when the absorbed energy is converted to the desired energy; and (3) the transmission stage when the energy is transferred to the end users. It is believed that the cost of ocean wave energy will significantly reduce together with the levelized cost of energy if more energy is absorbed from the ocean waves by a single unit system. In this study, the authors introduce a new concept in which a heaving point absorber WEC's design is optimized by making it resonance with two different wave frequencies. The new WEC will self-adjust its inertia (weight) by ballasting and de-ballasting using seawater. This design will significantly increase the overall power capture of the device. Section 2

introduces the new design concept and its operation while Section 3 discusses the wave data used in this study and estimates the wave resource potential. The power capture of this new design is simulated and discussed in Section 4 while its structural performance and reliability is analyzed and presented in Section 5. The last section is conclusions.

2. The Proposed Self-Adjustable WEC Concept

Ocean Wave Data

In the proposed WEC design, a cylindrical buoy is made to oscillate vertically during its interaction with the ocean waves. It slides up and down through a fixed solid frame (Figure 1). The oscillating buoy is a hollow cylinder that has an inlet and an outlet equipped with one-way valves close to its base submerged in the sea. There is a circular plate inside the hollow cylinder that is held in place by a cable/spring attached to the inner wall of the cylinder. This plate is to prevent the spilling of water beyond the desired level during its operation. At a predetermined location in the cylinder, end stoppers are attached to restrict the movement of the plate inside the cylinder. A simple device, which is attached to an open/close valve, is placed below the sea surface several meters away from the frame and buoy to measure the ocean wave period. The valve will open when the wave period is above a certain determined critical period, and it will close when the wave period falls below the critical period. Connecting the ocean wave measuring system valve to the inlet of the oscillating buoy is a highly flexible pipe for transporting water into the buoy chamber. The depth of the chamber is determined by the difference in drafts of the buoy when it is empty and when it is filled with water. The design is made in such a way that water will flow through gravity into the buoy once the valve opens. The depth between the ocean wave measuring device and inlet of the buoy depends on the wave amplitude, the draft of the buoy and the maximum heave oscillation amplitude. In this study, the measuring device is 2 m below sea level while about 98% of the wave amplitude examined is below 2 m. This gives a depth of 2.5 m between the inlet of the buoy and the measuring device during stage 1 when the draft is 4.5 m. The highest oscillation expected at this point has about 1.8 m amplitude. Hence, water can still flow to the buoy chamber during its operation. The proposed concept will increase the draft and subsequently the weight of the buoy between two resonance bandwidths by adding water into the buoy.

From Equation (2), the resonant period of a typical mass-spring system that is similar to a heaving buoy at sea is given as

$$\omega_n = \sqrt{\frac{\rho g S + K}{m + A}} \tag{2}$$

where, ω_n is resonance frequency, K is overall stiffness of system, A is added mass and m is mass of the buoy.

The operation of the proposed self-adjustable WEC is summarized in the following three stages.

Stage-1: The buoy's chamber is empty, and it is oscillating with respect to all ocean wave periods below the critical period. Both inlet and outlet valves of the buoy remain closed (Figure 2a).

Stage-2: The ocean wave period becomes equal or greater than the critical period. The valve connected to the ocean wave measuring device and the inlet valve of the buoy open. Sea water starts to flow into the buoy. Water enters into the chamber and pushes the steel plate up. The draft of the buoy starts increasing as the weight of the buoy increases. Taking seawater as an incompressible fluid, from Bernoulli's equation, the inlet water velocity V_{in} can be estimated using Equation (3)

$$V_{in} = \sqrt{2g(h - x - y)} \tag{3}$$

where, x is depth of ocean wave measuring device below sea surface, $h \in (0, h_{max})$ is buoy draft, h_{max} is draft of buoy at stage 2, $y \in (0, y_{max})$ is depth of water in chamber, y_{max} is depth of water in chamber at stage 2 and g is gravitational acceleration.
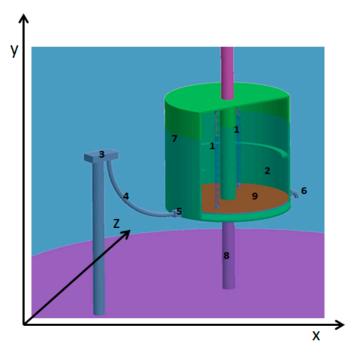
Figure 1. The conceptual design of the self-adjusted WEC with main components: 1. Cable/spring; 2. WEC chamber; 3. wave period measuring device and inlet valve to allow seawater flow into the flexible pipe through gravity; 4. flexible pipe; 5. WEC chamber inlet; 6. WEC chamber outlet; 7. WEC buoy; 8. frame; and 9. plate/diaphragm.
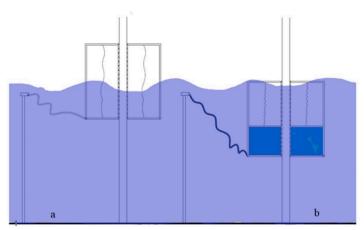

Figure 2. Stages of operation of the self-adjustable WEC.

Other formulas guiding the determination of the size of the inlet valve include Equation (4) for calculating the cross-sectional area A_{in}.

$$A_{in} = \frac{A_s y_{max}}{t V_{in}} \tag{4}$$

where, A_s = cross-sectional area of the buoy chamber and t = time to fill the chamber with sea water.

The stiffness of the cable spring is given as Equation (5) below

$$P = \rho g - \frac{m_s g}{y_{max}} \tag{5}$$

where, P is cable/spring stiffness and m_s is mass of the steel plate.

When water reaches the maximum point in the chamber, stage 2 is complete and the buoy starts to oscillate at periods greater than or equal to the critical period (Figure 2b).

Stage-3: The ocean wave period falls below the critical period. Outlet valve on the buoy opens, and water flows out of the buoy under the pressure of cable springs. Weight and draft of the buoy reduces until it returns back to stage 1 (Figure 2a). Buoy oscillates with respect to ocean wave's period less than the critical period. The outflow velocity of water V_{out} can be estimated using Equation (6)

$$V_{out} = \sqrt{2\left(\frac{M_s g}{\rho A_w}\right) + \frac{Py}{A_s \rho} + gy} \qquad (6)$$

One of the advantages of this new concept is that the inertia change of the WEC is achieved by ballasting and de-ballasting with sea water. The water is expected to flow in and out of the buoy mainly through gravity without any input of external power. The critical parts of the buoy are the inlet and outlet valves situated on the buoy. To determine the minimum and maximum flow rate the valves will experience for selecting the right capacity range of the valves, a series of optimization processes (Figure 3) are conducted based on Equations (3)–(6). The optimization processes are conducted using Simulink application in MATLAB software. Input parameters are determined from the combination of data in Section 3 and analyses in Section 4, such as the buoy draft, buoy chamber depth, cross sectional area of the buoy chamber from the buoy diameter, etcetera. These values form the inputs into the optimization processes to determine the flow rates for the inlet and outlet valves. In this study, the maximum time needed for the buoy to be filled or emptied is estimated as 5 min.
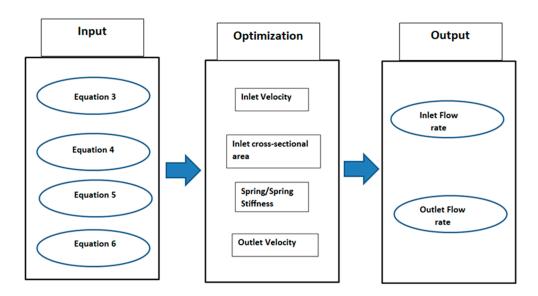

Figure 3. Optimization process for the buoy.

3. Ocean Wave Data and Resource Assessment

Ocean wave data including significant wave heights and wave periods are collected and analyzed over a nine year period from a selected location in the Gulf of Mexico close to Texas [25] (Figure 4). The weather buoy from which the data is obtained is operated by the National Data Buoy Center in a location with sea depth of 84 m and coordinates of (26.968N, 96.693W). The ocean wave data is recorded every hour. Data analysis results (Table 1) show that 99% of the waves occur between 3 and 12 s wave period with a 1–5 m wave height. The data also shows that the most prevalent significant wave periods lie between 5 and 6 s and 6 and 7 s. Hence, the proposed WEC design described in Section 2 is made to resonate at 5–6 s and 6–7 s through the inertia change to increase its power performance.

Figure 4. Weather buoy location.

Table 1. Percentage ocean wave height and period occurrence.

		Significant Wave Height (m)				
		0–1	1–2	2–3	3–4	4–5
	0–1	0.37%	0.00%	0.00%	0.00%	0.00%
	1–2	0.00%	0.00%	0.00%	0.00%	0.00%
	2–3	0.80%	0.06%	0.01%	0.01%	0.00%
	3–4	4.14%	0.31%	0.06%	0.01%	0.00%
	4–5	8.26%	2.86%	0.19%	0.02%	0.00%
Dominant Wave Period (s)	5–6	12.91%	12.55%	0.80%	0.09%	0.03%
	6–7	6.49%	14.54%	2.64%	0.17%	0.01%
	7–8	3.64%	12.47%	5.33%	0.79%	0.03%
	8–9	1.03%	2.60%	2.02%	0.54%	0.04%
	9–10	0.48%	1.09%	0.91%	0.31%	0.06%
	10–11	0.17%	0.37%	0.23%	0.10%	0.04%
	11–12	0.02%	0.02%	0.04%	0.03%	0.01%

Ocean wave power density can be estimated using Equation (7) under deepwater scenario, and the annual energy potential can be estimated by multiplying the power density with the percentage occurrence within one year interval. The annual energy potential result is given in Table 2 with a total annual energy potential of 105.3 MWh/m·y.

$$P_w = \frac{\rho g^2 T_e H^2}{64\pi} \tag{7}$$

where P_w (kW/m) is power density (power per unit width of wave front), ρ (kg/m^3) is seawater density, g (m/s^2) is gravitational acceleration, T_e (s) is energy wave period and H (m) is significant wave height.

Table 2. Annual energy resource potential (kWh/m·y) based on hourly resolution data.

		Significant Wave Height (m)				
		0–1	1–2	2–3	3–4	4–5
	2–3	92.76	27.64	14.55	16.47	0.00
	3–4	640.40	188.96	86.45	15.68	0.00
	4–5	1594.86	2206.21	324.17	66.65	0.00
	5–6	2991.75	11,637.70	1664.51	343.43	161.71
Dominant Wave Period T(s)	6–7	1754.96	15,724.72	6430.88	719.00	34.30
	7–8	1124.37	15,411.87	14,819.10	3895.31	235.22
	8–9	357.25	3613.04	6323.26	2992.05	363.86
	9–10	184.75	1689.70	3153.47	1921.00	600.31
	10–11	73.31	636.08	897.53	698.62	471.67

4. Design of Wave Energy Converter

The design processes of the proposed WEC consist of two steps. Firstly, the dimensions of the WEC are estimated using theoretical hydrodynamics of floating bodies where the motion and reactions of a floating body to external ocean wave forces are determined. The set of equations and processes to determine these initial dimensions were described in [19]. The initial dimensions of the WEC with 0.15 m thickness across different diameters using steel as the material are shown in Table 3. Based on the data shown in Table 3, the buoy would float naturally in sea water when its diameter is 5 m or larger.

Table 3. Draft for different diameters and wave period to achieve resonance (density of material = density of steel).

		Diameter (m)										
		1.3	2	3	4	5	6	7	8	9	10	11	12
	3–4	1.2	1.7	2.3	2.8	3.3	3.6	3.9	4.1	4.1	4.1	4.0	3.8
	4–5	1.9	2.7	3.8	4.9	5.8	6.6	7.4	8.0	8.6	9.1	9.5	9.7
Dominant Wave Period (s)	5–6	2.8	4.0	5.7	7.3	8.8	10.3	11.6	12.9	14.0	15.1	16.1	17.0
	6–7	3.8	5.5	7.9	10.2	12.5	14.6	16.6	18.6	20.5	22.2	23.9	25.5
	7–8	5.0	7.3	10.5	13.6	16.6	19.6	22.4	25.2	27.9	30.5	32.9	35.3
	8–9	6.3	9.3	13.4	17.4	21.4	25.2	29.0	32.7	36.3	39.8	43.2	46.5

After the initial dimensions are decided, the dimensions associated with 8 m diameter buoy are used as inputs into ANSYS/AQWA suite version 18.1 for a more detailed hydrodynamic diffraction analysis to determine the draft of the buoy, so that the buoy will experience resonance under the two most critical wave periods as determined in Section 3. With the draft and dimensions finalized (see Table 4), the operation process of the proposed self-adjustable WEC can be simulated to get its power performance and structure analysis results. The result from the detailed diffraction analysis in ANSYS/AQWA (Figure 5) shows that the two levels of the response amplitude operator (RAO) when resonance period as 5.5 s and 6.5 s, respectively. Figure 5 also shows the RAO of the proposed self-adjustable WEC with the critical period as 6 s.

Table 4. Operation level of the self-adjustable wave energy converter.

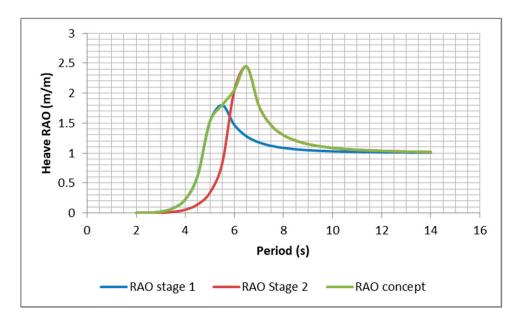| Stage	Draft (m)	Resonance Period
1	4.5	5.5
2	7.3	6.5

Figure 5. RAO curves of the WEC at Stage 1 (resonant period as 5.5 s), Stage 2 (resonant period as 6.5 s), and the proposed self-adjustable WEC with critical wave period as 6.0 s.

The inertia (weight) of the self-adjustable WEC changes during operation as the ocean wave period crosses the critical wave period that is 6 s for this study. The drafts and resonance periods of the two stages of operation are shown in Table 4 below. The diameter of the buoy is 8 m and the depth of the buoy is also 8 m. When the ocean wave period is less than 6 s, the buoy operates at stage 1. When the ocean wave period is above 6 s, it operates at stage 2.

5. Power Capture of the Wave Energy Converter

The estimated annual energy capture of the self-adjustable wave energy converter is simulated using ANSYS/AQWA hydrodynamic diffraction and hydrodynamic response suite. The response analysis is computed in the time domain including the device force, velocity, acceleration, displacement, etc. The power capture is estimated through the combinations of the heave response analysis. Since hourly ocean wave data is used in this paper, it is assumed that the ocean wave significant wave height and dominant wave period remain constant within this time frame (one hour).

The power take-off in this study is modeled as pure damper that is assumed to be frequency dependent. The motion equation of the heaving point absorber buoy with the PTO can be described by Equation (1) above. Therefore are PTO behaving as a pure damper will have the equation below

$$F_{PTO} = D_{PTO}\dot{x} \tag{8}$$

where, F_{PTO} is the PTO force and D_{PTO} = PTO damping coefficient.

The maximum amount of energy captured by the buoy occurs when the PTO damping is equal to the radiation damping of the buoy [26]. Hence, the PTO damping will be equal to that of the buoy at resonance. The mean absorbed power by the PTO is given by Equation (9),

$$\frac{1}{2}D_{PTO}\omega_n^2 x^2 \tag{9}$$

where, ω_n is the angular frequency at resonance.

Using the premises highlighted above, different values of PTO damping are tested on the buoy and the results of power capture evaluated using equations 8 and 9 are shown in Figure 6. The maximum value occurred when the damping coefficient is 50kNm/s for both stage 1 and stage 2.
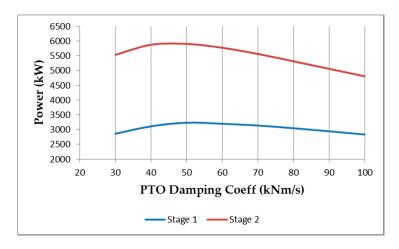
Figure 6. PTO damping vs. power capture.

The results of the annual energy capture of the proposed self-adjustable WEC is shown in Table 5, while Table 6 shows the annual energy capture by a non-self-adjustable WEC with similar dimensions designed to capture energy at the most prevalent wave period. The estimated total power capture for the non-self-adjustable WEC is 212 MWh/y while that of the self-adjustable WEC is 237 MWh/y. This shows a 12% annual increase. The results also show that the energy capture is the same when the wave period is below 6 s, which is the critical period for this design. However, there is considerable increase in energy capture when the wave period is above 6 s.

Table 5. Annual energy capture of the self-adjusted wave energy converter.

		Significant Wave Height (m)				
		0–1	1–2	2–3	3–4	4–5
	2–3	0.65	0.18	NA	NA	0.00
	3–4	214.31	60.68	26.02	NA	0.00
	4–5	8482.08	11,789.03	78.05	33.27	0.00
	5–6	14,458.04	56,266.15	8050.77	142.86	78.57
Dominant Wave Period T (s)	6–7	4688.81	41,987.27	17,153.00	1914.83	112.97
	7–8	1711.14	23,443.56	22,517.25	5908.53	467.93
	8–9	319.87	3239.32	5674.11	2685.95	429.93
	9–10	109.88	1006.56	1881.34	1147.69	463.03
	10–11	30.44	265.57	377.07	295.52	252.03

Table 6. Annual energy capture of the non-self-adjustable wave energy converter.

		Significant Wave Height (m)				
		0–1	1–2	2–3	3–4	4–5
	2–3	0.65	0.18	NA	NA	NA
	3–4	214.31	60.68	26.02	NA	NA
	4–5	8482.08	11,789.03	78.05	33.27	0.00
	5–6	14,458.04	56,266.15	8050.77	142.86	78.57
Dominant Wave Period T (s)	6–7	3748.43	33,556.00	13,694.89	1526.07	14.28
	7–8	1390.29	19,072.76	18,350.75	4825.71	291.48
	8–9	282.34	2882.82	5104.10	2448.30	302.44
	9–10	101.03	935.14	1776.91	1108.37	356.59
	10–11	28.56	251.38	362.04	289.27	201.52

6. Structural Analysis

The harsh ocean environment presents a challenge for the survival of WECs. A WEC must be able to withstand the forces thatit will be subjected to during its design life. A robust design becomes important because notable WEC projects have been abandoned due to the WECs' structural failure [27].

This challenge becomes more critical for point absorber WECs since they are usually designed to operate at resonance when most forces are experienced while most offshore structural systems are designed to operate away from their resonance bandwidth. The proposed self-adjustable WEC is designed to operate at two different resonance bandwidths, which makes the challenge to have a robust design even greater. Due to lack of commercialization, the WEC design has few recommended practices or technical specifications to follow. One of such specifications is the IEC TS 6200-2 [28]. Meanwhile, many relevant scholarly articles exist to be used as guidance and references. In addition, well developed and tested offshore standards created by offshore industrial companies and organizations, such as Det Norske Veritas (DNV) [29] and American Bureau of Shipping (ABS) [30], can also be used as guides for structural design of offshore systems including WECs.

Normally, any steel and other metallic structure operating in the ocean environment will be coated to prevent corrosion. In this study, it is assumed that the thickness of the buoy is decreased based on a predicted rate of corrosion. Different models and studies have been carried out to estimate the corrosion rate of steel in sea water [31–33]. In this study, the United States Army Corps of Engineers' corrosion rate on steel sheet of approximately 0.05–0.25 mm/y [34] is used. With a proposed design life of 30 years for the self-adjustable WEC and the upper limit of the range (0.25 mm/y), an additional layer of thickness of 7.5 mm is added to the proposed self-adjustable WEC design.

6.1. Extreme Wave Structural Analysis

In this study, ANSYS structural suite is used to perform the static structural analysis on the buoy and its interaction with the buoy frame. Ocean loads are obtained from the hydrodynamic, and time response analysis is applied on the buoy in the ANSYS structural static environment. The most probable highest loads are estimated from the 100-year return wave for the Gulf of Mexico [35] and used with guidance from DNV-OS-C201 [36] as the design waves to decide the highest forces and moments to be experienced by the buoy. Fatigue analysis is performed on the structure using cyclic loading from the loads expected to be experienced over the design life of the buoy. For the structural analysis, the highest forces and motions expected to be experienced by the buoy during extreme environmental conditions are applied. A multi-objective genetic algorithm (MOGA) tool in ANSYS is used to find the optimum design solutions for the heaving buoy that satisfies the structural requirements. The entire process is illustrated in Figure 7.
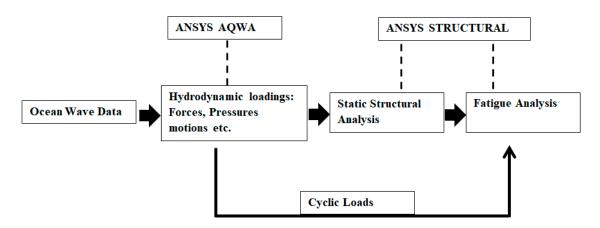
Figure 7. Structural design process.

A crossover rate of 0.95 and mutation rate of 0.05 are chosen when using the MOGA in ANSYS. The objective set for the analysis is to maximize the buoy's factor of safety. The inputs and their constraints are given as the buoy thickness with values between 0.1 m and 0.16 m, while friction coefficient between the buoy and the frame is set between 0.05 and 0.2. The evolution of the factor of safety is shown in Figure 8. The multi-objective genetic algorithm employed in this study achieved

convergence after 258 generations. The desired factor of safety can be benchmarked at any desired point and the associated buoy thickness at that level will be used for the design. For this study, a factor of safety of 5 is chosen for the design.
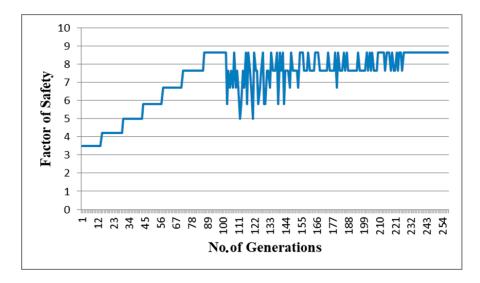

Figure 8. Buoy factor of safety evolution curve.

The structural analysis result (Figure 9) shows that the largest stresses are concentrated along the contact area between the buoy and the frame due to friction. This area is the most critical area of the buoy. The factor of safety evaluation by the software is based on the most critical parts that have the highest stresses. A safety factor equal to one means that the buoy is able to withstand the extreme forces that it is subjected to. When a safety factor is greater than one, the larger value of the safety factor means higher reliability of the structure. To increase the reliability, a safety factor no less than 5 is adopted for this study.
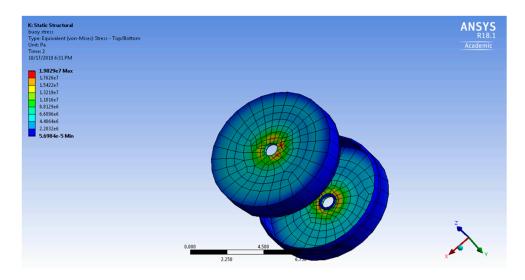

Figure 9. Extract from ANSYS showing stress distribution on buoy.

6.2. Fatigue Analysis

The deterministic method is used to analyze the fatigue response of the WEC device for a projected period of 30 years, which is the estimated operational life of the device. Discrete wave heights and periods with the corresponding number of occurrences are used for the analysis. These discrete wave

properties are used to generate the structural responses and hot spot stresses. The summation of the fatigue damages due to these discrete wave loads are then summed up to obtain the total damage during the life of the structure using steel's S–N curve (Figure 10).
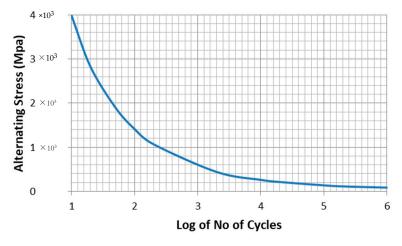

Figure 10. S–N curve of steel.

The discrete points used to determine the fatigue analysis of the WEC as shown in Table 7. It contains the sea states and the number of cycles of loadings associated with the sea states throughout the 30 years design life. The fatigue damage is provided in Table 8. The total fatigue damage is 0.2581 that is less than 1. Hence, the main structural parts will be able to withstand the cyclic loads during their design life.

Table 7. Sea states and number of stress cycles.

		Significant Wave Height (m)				
		0–1	1–2	2–3	3–4	4–5
	2–3	2082	155	36	23	0
	3–4	10,781	795	162	17	0
	4–5	21,480	7428	485	56	0
	5–6	33,578	32,654	2076	241	73
Dominant Wave Period (s)	6–7	16,883	37,818	6874	432	13
	7–8	9464	32,432	13,860	2049	79
	5–9	2673	6758	5257	1399	109
	9–10	1244	2845	2360	809	162
	10–11	449	974	611	267	116

Table 8. Sea states and damages.

		Significant Wave Height (m)				
		0–1	1–2	2–3	3–4	3–5
	2–3	0.0021	0.0002	0.00004	0.00002	0.0000
	3–4	0.0108	0.0008	0.00016	0.00002	0.0000
	4–5	0.0215	0.0074	0.00049	0.00006	0.0000
	5–6	0.0336	0.0327	0.00208	0.00024	0.0001
Dominant Wave Period (s)	6–7	0.0169	0.0378	0.00687	0.00043	0.0000
	7–8	0.0095	0.0324	0.01386	0.00205	0.0001
	5–9	0.0027	0.0068	0.00526	0.00140	0.0001
	9–10	0.0012	0.0028	0.00236	0.00081	0.0002
	10–11	0.0004	0.0010	0.00061	0.00027	0.0001
				Total damage		0.2581

7. Conclusions

In this study, we have introduced a new concept of wave energy converter based on a heaving point absorber system. The concept is based on modifying the inertia of the WEC through ballasting and de-ballasting using sea water so that it can interact at resonance with two different ocean waves' frequencies. The main objective is to increase the WEC's energy capture. Simulation results performed using ANSYS show that the annual energy captured by the proposed self-adjustable WEC is about 12% higher than a non-self-adjustable WEC with similar dimensions while using ocean wave data from a location in the Gulf of Mexico. Structural analysis is conducted to assess the survivability of the proposed WEC during its design life. Static structural analysis is performed on the self-adjustable WEC to determine its response when it is subjected to extreme wave conditions. Then, fatigue analysis is performed to determine whether the device can withstand the cyclic loads that it will be subjected to during its design life.

It is expected that ocean wave energy may become profitable and be competitive with other forms of energy such as wind and solar if more energy could be captured per unit device at the absorbing stage of ocean wave energy conversion process [8,37]. In this study, the authors only analyzed a unit wave energy converter. To effectively capture energy, future studies will incorporate the study of multiple arrays of the proposed WECs, and will consider wave wake effects on resource assessment, energy capture, structural response, etc. In addition, future study will also consider the entire ocean wave energy conversion processes including the absorbing, conversion and transmission with the proposed self-adjustable WEC concept, so that it will give a clearer picture in estimating the total economic costs of the self-adjustable WEC and a more reasonable comparison with other types of WECs.

References

1. Masters, C.D.; Root, D.H.; Dietzman, W.D. Distribution and quantitative assessment of world crude-oil reserves and resources. In *The Changing Carbon Cycle*; Springer: New York, NY, USA, 1986; pp. 491–507.
2. McGlade, C.; Ekins, P. The geographical distribution of fossil fuels unused when limiting global warming to 2 C. *Nature* **2015**, *517*, 187–190. [PubMed]
3. Grove-Palmer, C.O.J. Wave energy in the United Kingdom: A review of the programme June 1975 to March 1982. In Proceedings of the 2nd International Symposium on Wave Energy Utilization, Trondheim, Norway, 22–24 June 1982; pp. 22–24.
4. Previsic, M.; Moreno, A.; Bedard, R.; Polagye, B.; Collar, C.; Lockard, D.; Toman, W.; Skemp, S.; Thornton, S.; Paasch, R.; et al. Hydrokinetic energy in the United States—resources, challenges and opportunities. In Proceedings of the 8th European Wave Tidal Energy Conference, Uppsala, Sweden, 7–10 September 2009; pp. 76–84.
5. Thorpe, T.W. *A Brief Review of Wave Energy*; Harwell Laboratory, Energy Technology Support Unit: London, UK, 1999.
6. Wuebbles, D.J.; Jain, A.K. Concerns about climate change and the role of fossil fuel use. *Fuel Process. Technol.* **2001**, *71*, 99–119. [CrossRef]
7. Cruz, J. *Ocean Wave Energy: Current Status and Future Prespectives*; Springer Science & Business Media: Berlin/Heidelberg, Germany, 2007.

8.   Aderinto, T.; Li, H. Ocean wave energy converters: Status and challenges. *Energies* **2018**, *11*, 1250. [CrossRef]

9.   Ocean Energy Systems. Annual Report Ocean Energy Systems 2016. 2017. Available online: https://report2016.ocean-energy-systems.org/ (accessed on 11 March 2019).

10.   Best, R.; Burke, P.J. Adoption of solar and wind energy: The roles of carbon pricing and aggregate policy support. *Energy Policy* **2018**, *118*, 404–417. [CrossRef]

11.   Lehmann, M.; Karimpour, F.; Goudey, C.A.; Jacobson, P.T.; Alam, M.R. Ocean wave energy in the United States: Current status and future perspectives. *Renew. Sustain. Energy Rev.* **2017**, *74*, 1300–1313. [CrossRef]

12.   Available online: http://www.emec.org.uk/about-us/wave-clients/pelamis-wave-power/ (accessed on 20 September 2018).

13.   Astariz, S.; Iglesias, G. The economics of wave energy: A review. *Renew. Sustain. Energy Rev.* **2015**, *45*, 397–408. [CrossRef]

14.   Coe, R.G.; Yu, Y.H.; Van Rij, J. A survey of wec reliability, survival and design practices. *Energies* **2018**, *11*, 4. [CrossRef]

15.   Maples, B.; Saur, G.; Hand, M.; van de Pieterman, R.; Obdam, T. *Installation, Operation, and Maintenance Strategies to Reduce the Cost of Offshore Wind Energy*; National Renewable Energy Lab: Golden, CO, USA, 2013.

16.   Bachynski, E.E.; Young, Y.L.; Yeung, R.W. Analysis and optimization of a tethered wave energy converter in irregular waves. *Renew. Energy* **2012**, *48*, 133–145. [CrossRef]

17.   Budar, K.; Falnes, J. A resonant point absorber of ocean-wave power. *Nature* **1975**, *256*, 478–479. [CrossRef]

18.   Mei, C.C. Power extraction from water waves. *J. Ship Res.* **1976**, *20*, 63–66.

19.   Shadman, M.; Estefen, S.F.; Rodriguez, C.A.; Nogueira, I.C. A geometrical optimization method applied to a heaving point absorber wave energy converter. *Renew. Energy* **2018**, *115*, 533–546. [CrossRef]

20.   Goggins, J.; Finnegan, W. Shape optimisation of floating wave energy converters for a specified wave energy spectrum. *Renew. Energy* **2014**, *71*, 208–220. [CrossRef]

21.   Babarit, A.; Duclos, G.; Clément, A.H. Comparison of latching control strategies for a heaving wave energy device in random sea. *Appl. Ocean Res.* **2004**, *26*, 227–238. [CrossRef]

22.   Salter, S.H.; Taylor, J.R.M.; Caldwell, N.J. Power conversion mechanisms for wave energy. *Proc. Inst. Mech. Eng. Part M J. Eng. Marit. Environ.* **2002**, *216*, 1–27. [CrossRef]

23.   Li, G.; Weiss, G.; Mueller, M.; Townley, S.; Belmont, M.R. Wave energy converter control by wave prediction and dynamic programming. *Renew. Energy* **2012**, *48*, 392–403. [CrossRef]

24.   Zhang, X.; Tian, X.; Xiao, L.; Li, X.; Chen, L. Application of an adaptive bistable power capture mechanism to a point absorber wave energy converter. *Appl. Energy* **2018**, *228*, 450–467. [CrossRef]

25.   Available online: https://www.ndbc.noaa.gov/station_page.php?station=42020 (accessed on 13 November 2018).

26.   Falnes, J.; Perlin, M. Ocean waves and oscillating systems: Linear interactions including wave-energy extraction. *Appl. Mech. Rev.* **2003**, *56*, B3. [CrossRef]

27.   Times, V.H. Oceanlinx Energy Generator at Carrickalinga Is Still Considered Unsafe. 2014. Available online: https://www.victorharbortimes.com.au/story/2469811/oceanlinx-energy-generator-at-carrickalinga-is-still-considered-unsafe/ (accessed on 15 February 2020).

28.   IEC TS 62600-301:2019. *Marine Energy—Wave, Tidal and Other Water Current Converters-Part 301: River Energy Resource Assessment*; International Electrotechnical Commission: Geneva, Switzerland, 2019.

29.   Veritas, D.N. *DNV-RP-C205 Environmental Conditions and Environmental Loads*; Det Norske Veritas: Oslo, Norway, 2016.

30.   American Bureau of Shipping. *Design Standards for Offshore Wind Farms*; M10PC00105; American Bureau of Shipping: Houston, TX, USA, 2011.

31.   Paul, S. Estimation of corrosion rate of mild steel in sea water and application of genetic algorithms to find minimum corrosion rate. *Can. Metall. Q.* **2010**, *49*, 99–106. [CrossRef]

32.   Zayed, A.; Garbatov, Y.; Soares, C.G. Reliability of ship hulls subjected to corrosion and maintenance. *Struct. Saf.* **2013**, *43*, 1–11. [CrossRef]

33.   Zayed, A.; Garbatov, Y.; Soares, C.G. Corrosion degradation of ship hull steel plates accounting for local environmental conditions. *Ocean Eng.* **2018**, *163*, 299–306. [CrossRef]

34.   *U.S. Army Corps of Engineers. Engineering and Design: Department of the Army*; U.S. Army Corps of Engineers: Washington, DC, USA, 1994.

35. Marsooli, R.; Lin, N.; Emanuel, K.; Feng, K. Climate change exacerbates hurricane flood hazards along US Atlantic and Gulf Coasts in spatially varying patterns. *Nat. Commun.* **2019**, *10*, 1–9. [CrossRef] [PubMed]

36. Veritas, D.N. *DNV-OS-c201, Structure Design of Offshore Units (WESD Method)*; Det Norske Veritas: Oslo, Norway, 2011.

37. Aderinto, T.; Li, H. Review on Power Performance and Efficiency of Wave Energy Converters. *Energies* **2019**, *12*, 4329. [CrossRef]